

# Underwater Acoustic Communication Channel Capacity: A Simulation Study

Thomas J. Hayward and T. C. Yang

*Naval Research Laboratory, Washington, DC 20375*

**Abstract.** Acoustic communication channel capacity determines the maximum data rate that can be supported (theoretically) by an acoustic channel for a given source power and source/receiver configuration. In this paper, broadband acoustic propagation modeling is applied to estimate the channel capacity of a shallow water waveguide for a single source-receiver pair, both with and without source bandwidth constraints. Initial channel capacity estimates are obtained for a range-independent environment defined by the mean (time-averaged) sound speed profile measured at a site in the 1995 SWARM experiment. Without bandwidth constraints, estimated channel capacities approach 10 megabits per second at 1 km range, but after 2 km range they decay at a rate consistent with that of estimates by Pelloquin and Leinhos [1], which were based on a sonar equation analysis for a generic underwater channel. Channel capacities subject to source bandwidth constraints are approximately 30–90% lower than the upper bounds predicted by the sonar equation analysis, and exhibit a significant wind speed dependence. Simulations of internal wave effects on channel capacity show minimal effects at low frequencies but, at 2500 Hz, show a significant increase in the channel capacity at longer ranges. Implications for underwater acoustic communication systems are discussed.

## INTRODUCTION

Acoustic communication channel capacity determines the maximum data rate that can be supported (theoretically) by an acoustic channel for a given source power and source/receiver configuration. In practice, additional constraints are imposed on the source spectrum by the bandwidth limitations of physically realizable transducers. In this paper, broadband acoustic propagation modeling is applied to estimate the acoustic communication channel capacity of a shallow water waveguide as a function of range for a single source-receiver pair, both for unrestricted source bandwidth and for the limited bandwidths afforded by state-of-the-art transducers. We also present a preliminary examination, confined to a limited frequency band, of the effects of internal wave induced channel fluctuations on the channel capacity.

In early work in communication theory, the problem of determining the capacity of a linear communication channel with Gaussian source and perfectly known channel impulse response function was formulated as an extremal problem, leading to the explicit “waterfill” solution of [2]. Recent work has extended the determination of channel capacities to include simple channel models with, e.g., Rayleigh signal fading statistics. Significant work remains before these analyses can be extended to realistic representations of time-varying underwater acoustic channels.

The question of the maximum data rate has important practical implications. One would like to know what is theoretically possible and what causes degradation in the data rate. To obtain an upper bound on the channel capacity, we will assume that both the transmitter and receiver know the channel transfer function exactly for each transmission, and that the channel function does not vary during each transmission. These assumptions idealize the actual underwater acoustic communication scenario, in which there is a finite time, determined by the temporal coherence function, during which the channel transfer function varies minimally and can be learned, to considerable accuracy, through probe signals. The data rates of very short packets are experimentally measurable and can be compared with the theoretical channel capacity. The difference between the experimental and theoretical values can then provide a measure of the communication system performance.

## CHANNEL CAPACITY ESTIMATION

Reference 2 derives the capacity of a known time-invariant linear channel with transfer function  $H(f)$  for a Gaussian source having power spectral density  $X(f)$  and average power  $P$ , and additive Gaussian noise having power spectral density  $N(f)$ . In that case, the channel capacity is obtained as the maximum of the integral

$$I = \int_0^{\infty} \log_2 \left( 1 + \frac{H(f)X(f)}{N(f)} \right) df, \quad (1)$$

subject to the source power constraint

$$\int_{-\infty}^{\infty} X(f) df = P. \quad (2)$$

By a straightforward application of the method of Lagrange multipliers, the maximum is obtained when the source spectrum satisfies

$$X(f) = \max \left\{ L - \frac{N(f)}{H(f)}, 0 \right\}, \quad (3)$$

where the value  $L$  is chosen so that Equation (2) is satisfied. In acoustic communication, the channel capacity is a function of the source-receiver range through the (implicit) dependence of the acoustic transfer function  $H(f)$  on range.

Note that the optimal source spectrum defined by Equations (1) and (3) has the maximum spectral content supported by the channel, i.e., the set of all frequencies  $f$  for which  $L - N(f) / H(f) > 0$ . The bandwidth of this optimal source may, in fact, exceed that which is physically realizable by a single source transducer. In practice, the bandwidth is often limited to a fraction of the carrier frequency, and the carrier frequency is often set to be inversely proportional to the square root of the receiver

range. Channel capacity subject to these constraints can be found by restricting the frequencies in Equations (1)–(3) to the specified frequency bands.

## COMPUTATIONS FOR A RANGE-INDEPENDENT MEDIUM

The first simulations reported here are for a range-independent shallow-water environment derived from yo-yo CTD measurements taken during the 1995 SWARM experiment. [3] Figure 1 shows the mean water-column and bottom sound speed profiles, based on two hours of yo-yo CTD data and geoacoustic measurements reported in [3].

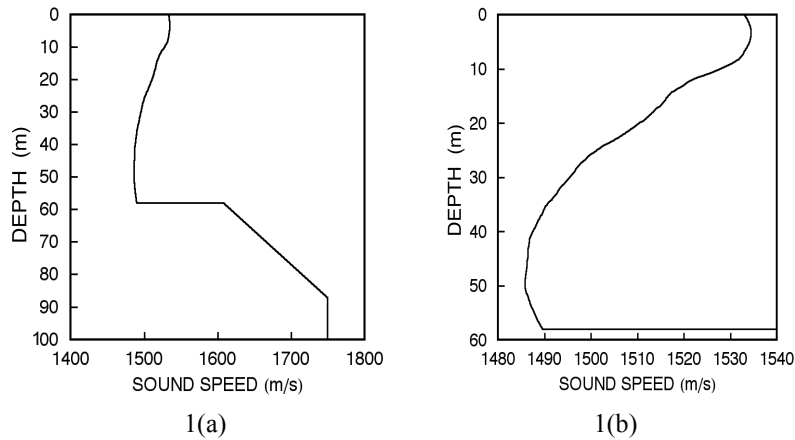


**FIGURE 1.** Mean sound speed profiles for the SWARM yo-yo CTD site: (a) water column, sediment and sub-bottom; (b) detail of water column.

Acoustic propagation losses were computed using a Gaussian-beam propagation code (Bellhop) [4] for a source at 10 m depth and a receiver at 30 m depth. Effects of bottom sound speed and attenuation were represented by reflection coefficients derived from the geoacoustic measurements. Surface scattering losses were computed using the SRFLOS component of the Oceanographic and Atmospheric Master Library (OAML) [5] for wind speeds of 3 kts, representing the upper end of Sea State 0, and 20 kts, representing Sea State 4. Volume attenuation was represented by Thorp's Law. [6] The ambient noise spectrum was constructed based on typical shallow-water noise spectra given in [7]. The acoustic fields were computed for frequencies ranging from 100 Hz to slightly less than 1 MHz in increments of 1/14 octave. This upper frequency limit was found to be sufficiently high to achieve the channel capacity in the simulations for ranges greater than 1.2 km.

### Results for Unconstrained Source Bandwidth

Figure 2 shows the noise-to-channel function ratio  $N(f)/H(f)$  and the optimum source spectral density  $X(f)$  for a source power of 193 dB  $\mu\text{Pa}^2$  and receiver ranges of 2, 5, 10 and 20 km. The upper frequency limits of the optimal spectra are

approximately 90, 40, 23, and 20 kHz, respectively. Because of the high signal to noise ratio for the 193 dB source, the optimal spectrum is nearly flat, eliminating the need for a “shaped” source spectrum.

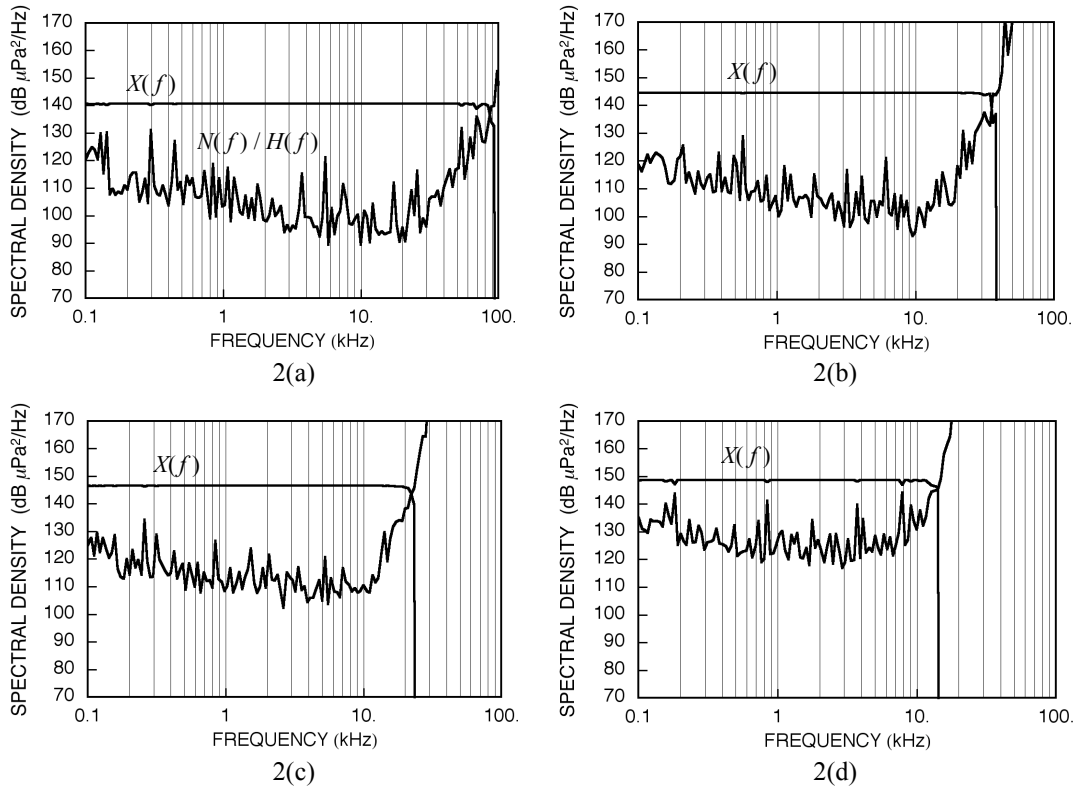


**FIGURE 2.** Noise-to-channel function ratio  $N(f)/H(f)$  and optimal signal power spectral density  $X(f)$  for ranges of (a) 2 km, (b) 5 km, (c) 10 km, and (d) 20 km. The source power is 193 dB  $\mu\text{Pa}^2$ , the source depth is 10 m, and the receiver depth is 30 m.

Note that the optimal source spectra most likely contain energy at frequencies below the lower frequency limit of 100 Hz used in the computations. Inclusion of these frequencies would increase the estimated channel capacity very slightly (by less than 1%). In practice, however, high-bandwidth systems would not likely include low frequencies in the transmitted spectrum.

Figures 3(a),(b) show the computed channel capacity for the mean sound speed profile as a function of range for wind speeds of 3 kts and 20 kts, respectively. The effect of the higher wind speed is to decrease the channel capacity by approximately 30–60%, except for certain ranges, at which waterborne paths most likely dominate the acoustic field. Note again that these estimates are based on the assumption of a perfectly known channel function, and thus represent upper bounds rather than practically achievable data rates.

The channel capacity estimates in Figs. 3(a),(b) assume full utilization of the available bandwidth in constructing the optimal source spectrum  $X(f)$  given by Equations (1)-(3). In practice, the bandwidth of a single transducer is limited to some

fraction of the carrier frequency. (Note, however, that the theoretical capacity could be approached by using multiple transducers.)

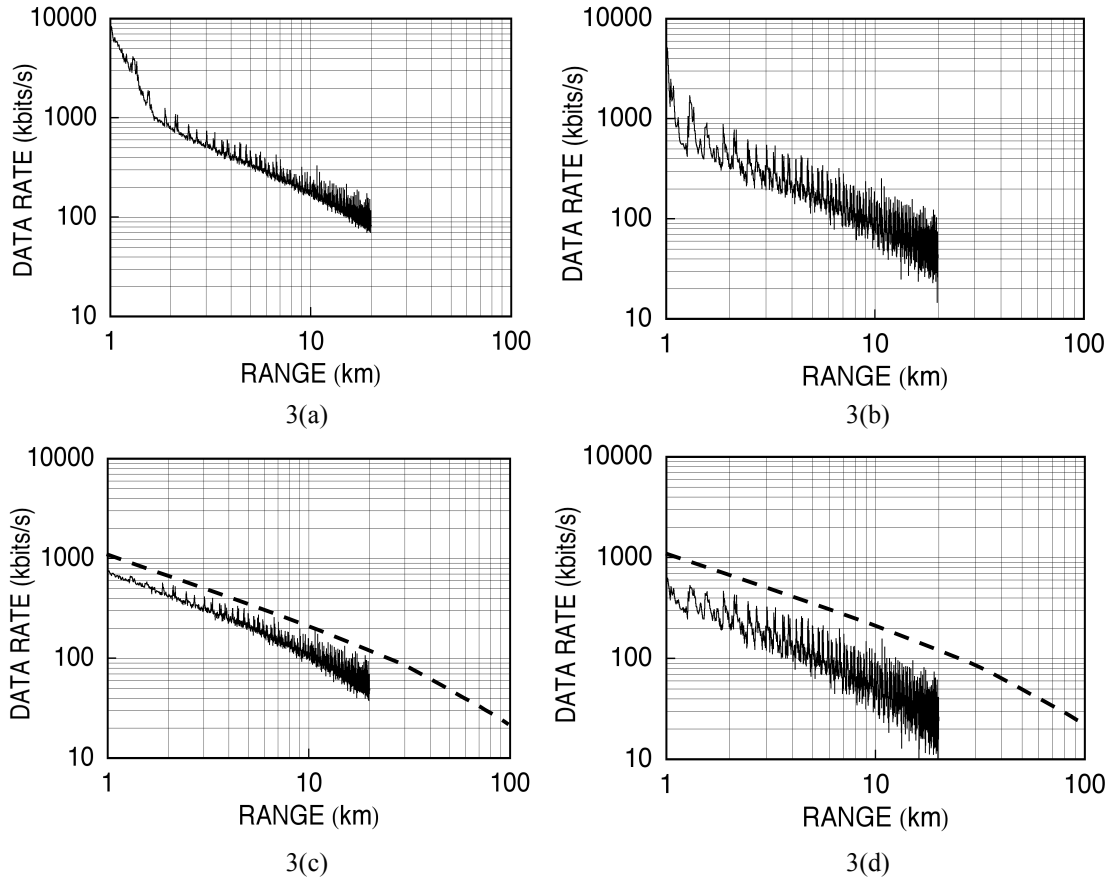


**FIGURE 3.** Solid curves: Channel capacity estimates for the mean sound speed profile at the SWARM yo-yo CTD site for source power  $193 \text{ dB } \mu\text{Pa}^2$ , source depth 10 m and receiver depth 30 m. (a) Unconstrained bandwidth, 3 kt wind speed. (b) Unconstrained bandwidth, 20 kt wind speed. (c) Constrained bandwidth, 3 kt wind speed. (d) Constrained bandwidth, 20 kt wind speed. Dashed curves: Channel capacity upper bounds for Sea State 0, subject to bandwidth equal to carrier frequency, obtained by Peloquin and Leinhos [1] for a generic underwater channel based on sonar-equation analysis.

### Results for Constrained Source Bandwidth

Channel capacities were computed assuming that the source bandwidth  $W$  equals the carrier frequency, and that the carrier frequency is given by  $F_c = a/\sqrt{r}$ , where  $a$  is determined by  $F_c = 20 \text{ kHz}$  at range  $r = 5 \text{ km}$ . Figs. 3(c) and 3(d) show the channel capacities calculated for the mean sound speed profile at the SWARM site, subject to the frequency band constraints, for wind speeds of 3 kts and 20 kts, respectively. Also shown is the upper bound obtained by Peloquin and Leinhos [1] for Sea State 0, based on a sonar-equation analysis for a generic underwater channel, with bandwidth constrained to be equal to carrier frequency. The computed channel capacities for the

SWARM environment are approximately 30–90% below the sonar equation based upper bounds, depending on wind speed and range.

## CAPACITY VARIATION IN AN INTERNAL WAVE FIELD

This section examines the effect on channel capacity of random sound speed variations induced by (diffuse) internal gravity waves. Again, it is assumed that, for each transmission, both the source and receiver know the channel function. This corresponds in practice to transmissions with very short packet lengths. When longer-length packets are used, the achievable data rates will decrease unless the receiver processor is able to track the channel variation. Ideally, it would be desirable to be able to calculate the channel capacity in the case of an uncertain channel. However, the problem is extremely difficult, and explicit results are known only for a few simple statistical models of the channel variation that fall short of a realistic representation of a time-varying, multipath underwater acoustic channel.

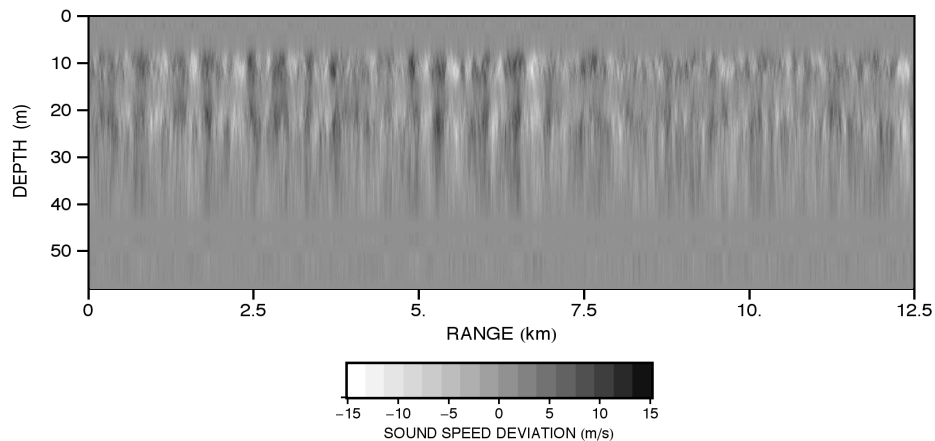


**FIGURE 4.** Sound speed deviation from the mean as a function of range and depth for a typical internal wave field realization.

Modeling acoustic propagation in a strongly range dependent medium requires extensive numerical computation. Because of the computation times required, this initial study examines the variations in channel capacity over limited frequency bands.

Realizations of linear internal wave fields were generated for the SWARM site, based on the spectrum of the internal waves derived from yo-yo CTD measurements taken at a time during which nonlinear internal waves were absent or negligible [3,8]. Figure 4 shows the sound speed deviation from the mean as a function of range and depth for a typical internal wave field realization. Geoacoustic properties were represented as described in the previous section.

Acoustic fields were computed using a parabolic equation code (RAM) [9] for frequencies of 300-400 Hz in increments of 1 Hz, for each of 200 realizations, and for frequencies of 900-1000 Hz for 100 realizations. Acoustic field computations for the 2500-2600 Hz band were based on a coupled normal mode model (C-SNAP) [10].

Figure 5 shows the mean values, over all of the realizations, of the ratios of the channel capacities of the internal-wave perturbed environments to the channel capacities of the mean environment, plotted as a function of range for frequency bands of 300-400 Hz and 900-1000 Hz. Assuming perfect knowledge of the channel, the effects of the internal waves on the channel capacity are minimal.

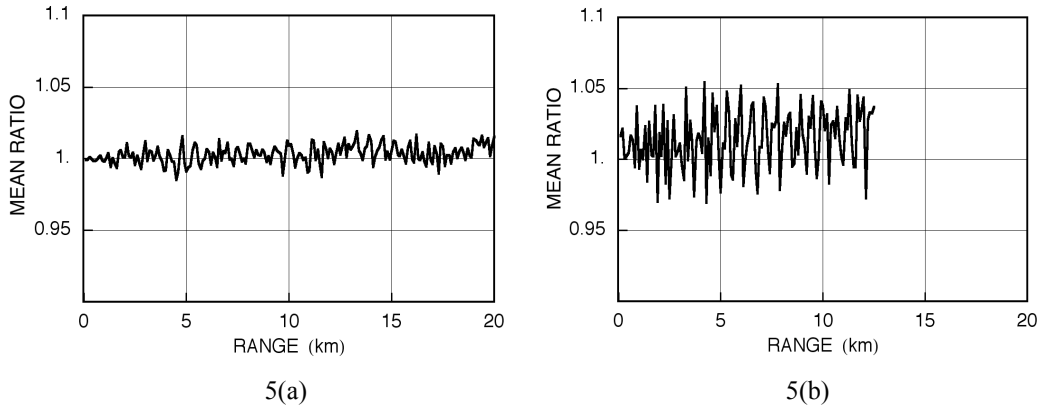


**FIGURE 5.** Mean values of the ratios of the channel capacities of the internal wave perturbed environments to the channel capacities of the mean environment, plotted as a function of range for frequency bands of (a) 300-400 Hz, and (b) 900-1000 Hz.

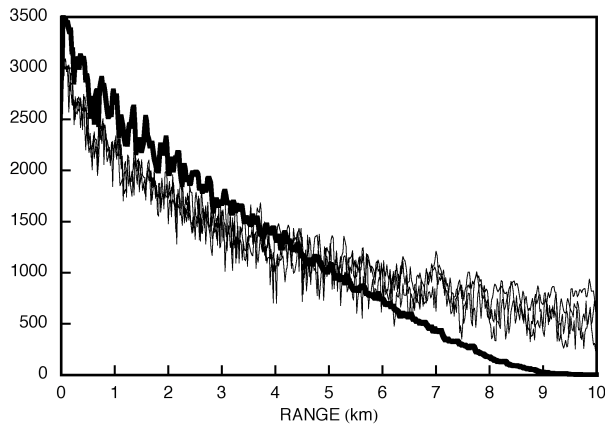


**FIGURE 6.** Heavy curve: Channel capacity for the mean environment for source power  $193 \text{ dB } \mu\text{Pa}^2$  and frequency constrained to 2500–2600 Hz. Light curves: Channel capacities for three realizations of the internal wave perturbed environment for the same frequency band.

Figure 6 shows the computed channel capacity for the mean environment for source power  $193 \text{ dB } \mu\text{Pa}^2$  and frequency constrained to 2500–2600 Hz (heavy curve). Also shown are the computed channel capacities for the same source power and frequency band for three realizations of the internal wave field. The effect of the internal waves is to enhance the acoustic field (hence the channel capacity) at longer ranges, but to decrease it at shorter ranges. These effects presumably result from the scattering of acoustic energy into lower propagation angles; this low-angle energy then propagates to longer ranges.

## SUMMARY AND DISCUSSION

Acoustic communication channel capacities were computed for a single source-receiver pair for a shallow water waveguide derived from the 1995 SWARM experiment, both for the range-independent mean environment and for the same environment perturbed by simulated linear internal wave fields. Without bandwidth constraints, estimated channel capacities for the mean environment approach 10 megabits per second at 1 km range for a source power of 193 dB  $\mu\text{Pa}^2$ . Channel capacities subject to commonly imposed source center frequency and bandwidth constraints are up to 90% lower at ranges less than 2 km. This suggests that further study of the optimal source frequency band as a function of range is warranted.

Effects of internal waves on theoretical channel capacity were examined in an initial study for limited (100-Hz) frequency bands centered at 350, 950 and 2550 Hz. Assuming that the channel is known, the internal waves had minimal effect on the channel capacity at the lower frequencies, but, for the 2500-2600 Hz band, the internal waves significantly increased the capacity at longer ranges, presumably due to scattering of acoustic energy into lower propagation angles.

The foregoing computations assume perfect knowledge of the channel function. Further study is needed to determine the extent to which the practically achievable data rates are limited by channel uncertainty, and to determine the optimal design of source spectra, coding, and signal processing to maximize the data rate.

## ACKNOWLEDGMENTS

This work was supported by the Office of Naval Research and by a grant of computer time from the Department of Defense High Performance Computing Modernization Program at the Army Research Laboratory Major Shared Resource Center. The authors thank Paul Gendron of NRL for helpful discussions.

## REFERENCES

1. Peloquin, R. F., and Leinhos, H., unpublished (1997).
2. Shannon, C. E., *Proc. IRE* **37**, 10-21 (1949).
3. Apel, J. H. et al., *IEEE J. Oceanic Eng.* **22**, 465-500 (1997).
4. Porter, M. B., and Bucker, H. P., *J. Acoust. Soc. Am.* **82**, 1349-1359 (1987).
5. Naval Oceanographic Office, OAML-SRS-37, Stennis Space Center, Mississippi, 1992.
6. Thorp, W. H., *J. Acoust. Soc. Am.* **42**, 270 (1967).
7. Urick, R. J., *Principles of Underwater Sound*, 3<sup>rd</sup> ed., McGraw-Hill, New York, 1983, p. 213.
8. Yang, T. C., and Yoo, K. B., *IEEE J. Oceanic Eng.* **24**, 333-345 (1999).
9. Collins, M. D., *J. Acoust. Soc. Am.* **93**, 1736-1742 (1993).
10. Ferla, C. M., Porter, M. B. and Jensen, F. B., SACLANTCEN Memorandum SM-274, LaSpezia, Italy, 1993.